Dalton Transactions

ROYAL SOCIETY OF CHEMISTRY

PAPER

View Article Online
View Journal | View Issue

Cite this: *Dalton Trans.*, 2020, **49**, 7790

$Li_2(Se_2O_5)(H_2O)_{1.5}{\cdot}CuCl_2$, a salt-inclusion diselenite structurally based on tetranuclear Li_4 complexes†

Mishel R. Markovski,[a] Oleg I. Siidra,*[a,b] Dmitri O. Charkin,[c] Victoria A. Vladimirova,[a] Alexander A. Tsirlin[d] and Vasili Yu. Grishaev[c]

Received 5th April 2020,
Accepted 10th May 2020

DOI: 10.1039/d0dt01260b

rsc.li/dalton

A new lithium copper diselenite chloride hydrate, $Li_2Se_2O_5(H_2O)_{1.5}{\cdot}CuCl_2$, was prepared from aqueous solution. Its unique 2D structure can be interpreted as $Li_2Se_2O_5(H_2O)_{1.5}$ layers with $CuCl_2$ hosts embedded in the interlayer space, and be considered halfway between the salt-inclusion and host–guest structures. The CuO_2Cl_4 octahedra form chains similar to those in $CuCl_2{\cdot}2H_2O$, yet water molecules are coordinated exclusively to Li^+ while $Se_2O_5^{2-}$ and Cl^- bridge Li^+ and Cu^{2+}. The complexity of the structure is likely responsible for both very long pre-crystallization time and non-existence of the corresponding bromide analogue. Despite the relatively long Cu···Cu separations, the compound exhibits weak ferromagnetic interactions along the chains of CuO_2Cl_4 octahedra.

Introduction

Combination of "lone-pair" cations (that is, p-block elements in intermediate valence states) and halide anions, acting as "chemical scissors", has been recognized as one of the most efficient instruments in constructing low-dimensional crystal structures.[1] These usually involve one or several types of cations adopting more regular arrangements, most commonly of d- or f-block elements that carry magnetic moments. Due to the relative ease of preparation, including single-crystal growth, compounds of lone-pair cations such as Pb^{II}, Sb^{III}, Bi^{III}, Se^{IV}, Te^{IV} and I^V, have been intensively studied in the last decades. The Se^{IV} compounds comprise an exception, though, as tetravalent selenium forms a variety of essentially chemically stable water-soluble species, *e.g.* selenious acid, hydroselenite anion, and SeX_6^{2-} complexes (where X = Cl or Br). Due to their relatively low solubility at ambient conditions, Se-based compounds were mostly prepared by solid-state, chemical transport, or hydrothermal routes.[2] Layered copper hydrogen selenites were studied in a number of works.[3–5] Recently, we have undertaken a thorough reinvestigation of the family of copper hydroselenite halides and nitrates of monovalent cations.[6,7] The most common stoichiometry observed was that of $(MX)[Cu(HSeO_3)_2]$ (M = Na, K, Rb, Cs, Tl, NH_4; X = Cl, Br, or NO_3); the structural architectures of such compounds are all based on the $[Cu(HSeO_3)_2]$ slab and depend on the size of the M^+ cation in the interlayer. No hints of similar compounds of the smallest alkali cation, Li^+, have been reported so far, probably because it lies beyond the tolerance limit of the $(MX)[Cu(HSeO_3)_2]$ motif. Nevertheless, crystals of novel $Li_2(Se_2O_5)(H_2O)_{1.5}{\cdot}CuCl_2$ with the crystal structure unrelated to that of $(MX)[Cu(HSeO_3)_2]$ were successfully obtained after a particularly long crystallization time.

Experimental

Synthesis

All initial attempts to prepare the lithium – copper hydroselenite halides started from the procedure similar to that employed earlier for the preparation of Na–Cs compounds.[6] 10 mmol of $CuCl_2{\cdot}2H_2O$ or $CuBr_2$ (Aldrich 99.8%) and 22 mmol of selenious acid (Aldrich 98%) were dissolved in 50 ml of distilled water; the initial turbidity was cleared by adding a few drops (0.1–0.2 ml) of trifluoroacetic acid (Vecton 99%). After that, 8 ml of saturated LiCl (LiBr) (both Aldrich 99.9%) solution was added. Upon evaporation, the solution color changed gradually to yellowish-green (Cl) or violet-brown (Br) indicating the formation of the corresponding CuX_4^{2-} complexes. The volume decrease due to evaporation ceased in approximately three weeks, and almost no changes were observed for several months afterwards. After this quite long period, large green crystals (Fig. 1) had formed within several hours in the chloride solution. The bromide solution

[a]*Department of Crystallography, St. Petersburg State University, University Emb. 7/9, 199034 St. Petersburg, Russia. E-mail: o.siidra@spbu.ru; Tel: +7 812 3506688*
[b]*Institute of Silicate Chemistry, Russian Academy of Sciences, Makarov Emb. 2, 199034 St. Petersburg, Russia*
[c]*Department of Chemistry, Moscow State University, Leninskie Gory 1, 119991 Moscow, Russia*
[d]*Experimental Physics VI, Center for Electronic Correlations and Magnetism, Institute of Physics, University of Augsburg, 86135 Augsburg, Germany*
†CCDC 1994941. For crystallographic data in CIF or other electronic format see DOI: 10.1039/d0dt01260b

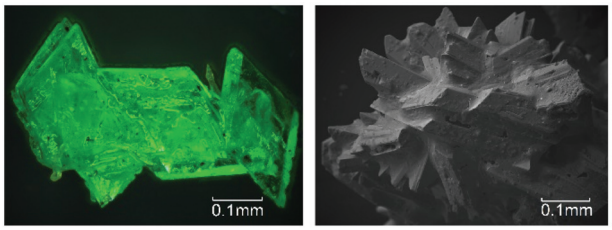

Fig. 1 Green crystals of $Li_2(Se_2O_5)(H_2O)_{1.5}{\cdot}CuCl_2$ under optical microscope (left) and BSE (backscattered electron) image (right).

was kept for some more time until it finally turned into a viscous black mass, which was discarded. When more concentrated chloride solutions were used, the overall crystallization time decreased to several weeks, yet rapid crystallization was still preceded by a long "incubation time". Attempts to hasten the crystal growth by gently heating the solution to 40–45 °C led to a reproducible formation of very unstable dark-red acicular crystals, which dissolved spontaneously upon cooling, and the crystals of $Li_2(Se_2O_5)(H_2O)_{1.5}{\cdot}CuCl_2$ subsequently appeared within a period of several hours to few days.

Crystals of $Li_2(Se_2O_5)(H_2O)_{1.5}{\cdot}CuCl_2$ are stable for months in the viscous mother liquor but deteriorate rapidly in air. There had been some problems in separating them from the viscous liquor upon sample preparation for spectroscopic and magnetic measurements. They immediately dissolve in cooled distilled water and turn dull in dried acetonitrile, which acquires a green color due to the presence of dissolved Cu^{2+} species. Most of the supernatant could be however removed by vacuum filtration, after which the crystals were placed on filter paper for just a few minutes for final drying.

Qualitative electron microprobe analysis (LINK AN-10000 EDS system) of $Li_2(Se_2O_5)(H_2O)_{1.5}{\cdot}CuCl_2$ revealed no elements with the atomic number greater than 11 (Na), other than Cl, Cu, and Se.

Single crystal XRD studies

A relatively large crystal of $Li_2(Se_2O_5)(H_2O)_{1.5}{\cdot}CuCl_2$ (*ca.* 0.35 × 0.29 × 0.20 mm) was mounted on a thin glass fiber using an epoxy glue which also protected the crystal from decay. The diffraction data were collected on a Bruker APEX II DUO X-ray diffractometer equipped with a micro-focus X-ray tube operated with MoKα radiation at 50 kV and 0.6 mA. More than a hemisphere of data was collected with a frame width of 0.5° in ω with 10 s counting time for each frame. The data were integrated and corrected for absorption using a multi-scan type model by Bruker programs APEX and SADABS. The structure was solved (Table 1) and refined using SHELXL software.[8] The final R_1 value of 0.03 was achieved for 1096 unique reflections with $|F_o| \geq 4\sigma_F$. The final model included anisotropic displacement parameters for all atoms, except of hydrogens that could nevertheless be localized. Selected bond distances and bond-valence values are given in Table 2.

Table 1 Crystallographic data and structure refinement parameters for $Li_2(Se_2O_5)(H_2O)_{1.5}{\cdot}CuCl_2$

a (Å)	13.075 (14)
b (Å)	7.672 (8)
c (Å)	17.79 (2)
β (°)	98.93 (3)
V (Å^3)	1763 (3)
Radiation	MoKα
Total reflections	9531
Unique reflections	1396
Unique $\lvert F_o \rvert \geq 4\sigma_F$	1096
Space group	$C2/c$
θ range	2.317–24.045
Crystal size (mm)	0.35 × 0.29 × 0.20
μ (cm^{-1})	11.332
D_{calc} (g cm^{-3})	3.114
GoF	1.030
R_1	0.03
R_1 (all data)	0.05

Table 2 Selected bond lengths (in Å) and bond-valence sums (BVS) in brackets (in valence units, vu) in the structure of $Li_2(Se_2O_5)(H_2O)_{1.5}{\cdot}CuCl_2$. The BVS for Li–O, Se–O and Cu–O bonds were calculated using parameters given by[27] and for Li–Cl, Cu–Cl bonds given by[28]

Li1–O4	1.912(15) [0.266]	Se2–O4	1.630(5) [1.532]
Li1–O2	1.943(15) [0.253]	Se2–O3	1.685(5) [1.340]
Li1–OW2	1.983(16) [0.238]	Se2–O5	1.817(5) [0.971]
Li1–O2	2.044(15) [0.217]	**BVS**	**3.84**
BVS	**0.97**		
Li2–O3	1.970(15) [0.243]	Cu1–O1	1.934(6) [0.499]
Li2–OW1	2.005(17) [0.230]	Cu1–O3	1.942(5) [0.488]
Li2–O1	2.027(17) [0.222]	Cu1–Cl1	2.294(3) [0.452]
Li2–O2	2.395(17) [0.125]	Cu1–Cl2	2.317(3) [0.425]
Li2–Cl2	2.599(17) [0.155]	Cu1–Cl2	2.787(2) [0.119]
BVS	**0.98**	Cu1–Cl1	3.116(3) [0.049]
Se1–O2	1.656(5) [1.438]	**BVS**	**2.03**
Se1–O1	1.680(5) [1.356]		
Se1–O5	1.788(5) [1.042]	H1–OW1	0.899(7) [1.046]
BVS	**3.84**	H2–OW2	0.886(7) [1.078]
		H3–OW2	0.899(9) [1.046]

IR spectroscopy

IR spectra of $Li_2(Se_2O_5)(H_2O)_{1.5}{\cdot}CuCl_2$ (Fig. 2) were obtained from powdered samples mixed with dried KBr, pelletized and analyzed at room temperature using a Bruker Vertex 70 FTIR spectrometer with a resolution of 4 cm^{-1}. The wavenumbers and intensities of most bands correspond to the $Se_2O_5^{2-}$

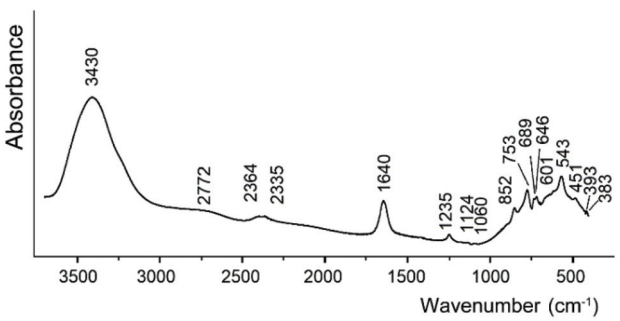

Fig. 2 Infrared (FTIR) spectrum of $Li_2(Se_2O_5)(H_2O)_{1.5}{\cdot}CuCl_2$.

anions.[9] An intensive and broad band at 3430 cm^{-1} indicates the presence of H_2O molecules. Two weak bands at 383 and 393 cm^{-1} may be attributed to the Cu–O stretching and O–Cu–O bending modes.[10]

Magnetic measurements

Magnetization measurements were performed on a *ca.* 10 mg polycrystalline sample of $Li_2(Se_2O_5)(H_2O)_{1.5}{\cdot}CuCl_2$ using the MPMS SQUID VSM magnetometer from Quantum Design in the temperature range of 1.8–400 K and in magnetic fields up to 7 T. The temperature dependence of magnetic susceptibility was recorded in fields of 0.1 T and 5 T upon heating the sample in both zero-field cooling (ZFC) and field-cooling (FC) regimes. Field-dependent magnetization was measured at 2 K, 50 K, 100 K, 300 K and 400 K.

Numerical simulations

Temperature-dependent susceptibility and field-dependent magnetization of the ferromagnetic spin-1/2 dimer and ferromagnetic spin-1/2 chain were obtained by quantum Monte-Carlo simulations using the *loop* and *dirloop_sse* algortihms of the ALPS simulation package.[11,12] For the spin chain, a finite lattice with $L = 48$ sites and periodic boundary conditions was used. Exchange parameters in the manuscript refer to the spin Hamiltonian defined as $H = \Sigma J S_i S_j$, where $S = \frac{1}{2}$ and the summation is over lattice bonds.

Results and discussion

Crystal structure

The $Se_2O_5^{2-}$ anions (Fig. 3) exhibit a typical geometry with the short Se–O_t (1.63–1.69 Å) and long Se–O_{br} distances (1.79–1.82 Å) (O_t = terminal oxygen; O_{br} = bridging oxygen) (Table 2). Both Se1 and Se2 atoms have $Se^{4+}O_3E$ pseudotetrahedral arrangements. The terminal O1 and O3 atoms form bonds to both Cu^{2+} and Li^+ while O2 and O4 bond only to Li^+.

The Li^+ cations are coordinated by both Cl^- and $Se_2O_5^{2-}$ anions as well as water molecules; the Li–O and Li–Cl distances are similar to those observed in the structure of $LiCl{\cdot}H_2O$.[13] The Li1 coordination environment can be described as a distorted $LiO_3(H_2O)$ trigonal pyramid with the Li1–O bonds in the range 1.91–2.04 Å, whereas the Li2 atom has a mixed-ligand coordination environment represented by the $LiO_3(H_2O)Cl$ trigonal bipyramid. The $LiO_3(H_2O)$ and $LiO_3(H_2O)Cl$ polyhedra share common oxygen atoms, thus forming a $\square Li_4$ tetrahedral cavity in the center (Fig. 3). It is worth noting that the water molecules are bonded exclusively to Li^+. The water molecules polarized by Li^+ form typical hydrogen bonds to both oxygen and chlorine atoms. However, this is not entirely surprising as the Cu^{2+} cations with the higher charge interact exclusively with the anions, so the Coulombic energy adds to the overall stability of the structure.

The CuO_2Cl_4 octahedra exhibit a strong Jahn–Teller distortion with the more ionic Cu–Cl bonds strongly affected. Each Cl^- forms one short and one long bond to the neighboring Cu^{2+} cations. The $Cu^{2+}{\cdots}Cu^{2+}$ distances of 3.581(4) Å suggest the absence of direct interactions between the magnetic ions.

The Li-centered polyhedra linked *via* diselenite groups form blocks depicted in Fig. 4a. The CuO_2Cl_4 octahedra share common Cl1–Cl1 and Cl2–Cl2 edges, thus forming chains in the interlayer (Fig. 4b). The chains are very similar to those observed in the structure of $CuCl_2{\cdot}2H_2O$[14] except that in $Li_2(Se_2O_5)(H_2O)_{1.5}{\cdot}CuCl_2$ the oxygen atoms belong not to water molecules, but are strongly bonded in diselenite groups. The structure of $Li_2(Se_2O_5)(H_2O)_{1.5}{\cdot}CuCl_2$ can be described as based on electroneutral $\{Li_2(Se_2O_5)(H_2O)_{1.5}\}$ blocks with $(CuCl_2)$ species inserted in between (Fig. 4c and d). 'Lone pairs' of Se^{4+} point in the direction of Cl^- ions; the Se···Cl distances of 3.240(4) Å can be considered as non-bonding.

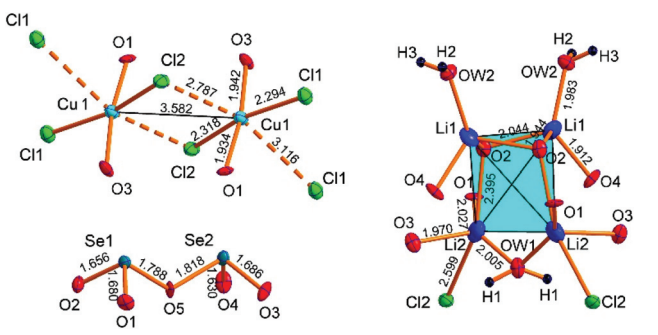

Fig. 3 Coordination environments of cations in the structure of $Li_2(Se_2O_5)(H_2O)_{1.5}{\cdot}CuCl_2$. Li_4 tetrahedral cavity is highlighted by blue.

Magnetic properties

Temperature dependence of the molar magnetic susceptibility for $Li_2(Se_2O_5)(H_2O)_{1.5}{\cdot}CuCl_2$ is shown in Fig. 5. Weak curvature of the inverse susceptibility can be ascribed to a small temperature-independent contribution superimposed on the Curie-like paramagnetic behavior. A modified Curie–Weiss fit with $\chi = \chi_0 + C/(T - \theta)$ above 50 K returns $\chi_0 = -1.67 \times 10^{-4}$ emu mol^{-1}, C = 0.475 emu K mol^{-1}, and $\theta = 0$ K. This temperature-independent contribution is almost exclusively due to core diamagnetism, $\chi_{dia} = -1.54 \times 10^{-4}$ emu mol^{-1} estimated using Pascal's constants.[15] The Curie-constant C is slightly higher than expected for a spin-1/2 ion (C = 0.375 emu K mol^{-1}) and corresponds to the paramagnetic effective moment of $\mu_{eff} = 1.95\mu_B$ with the g-value of $g = 2.25$, which is in the typical range for Cu^{2+} ions.[16]

At first glance, the vanishing Curie–Weiss temperature would indicate the absence of any sizable magnetic interactions between the Cu^{2+} ions. However, a closer look at the low-temperature data (Fig. 5) reveals conspicuous deviations from the Curie law for the 0.1 T data below 15 K. Similar deviations are seen in the magnetization curve at 2 K that does not follow the Brillouin function expected for paramagnetic spin-1/2 ions (Fig. 6). Magnetization of $Li_2(Se_2O_5)(H_2O)_{1.5}{\cdot}CuCl_2$ saturates faster than that of a paramagnet, whereas low-temperature susceptibility shows positive deviation from the Curie law. Both observations indicate weak but non-negligible ferromagnetic interactions between the Cu^{2+} ions.

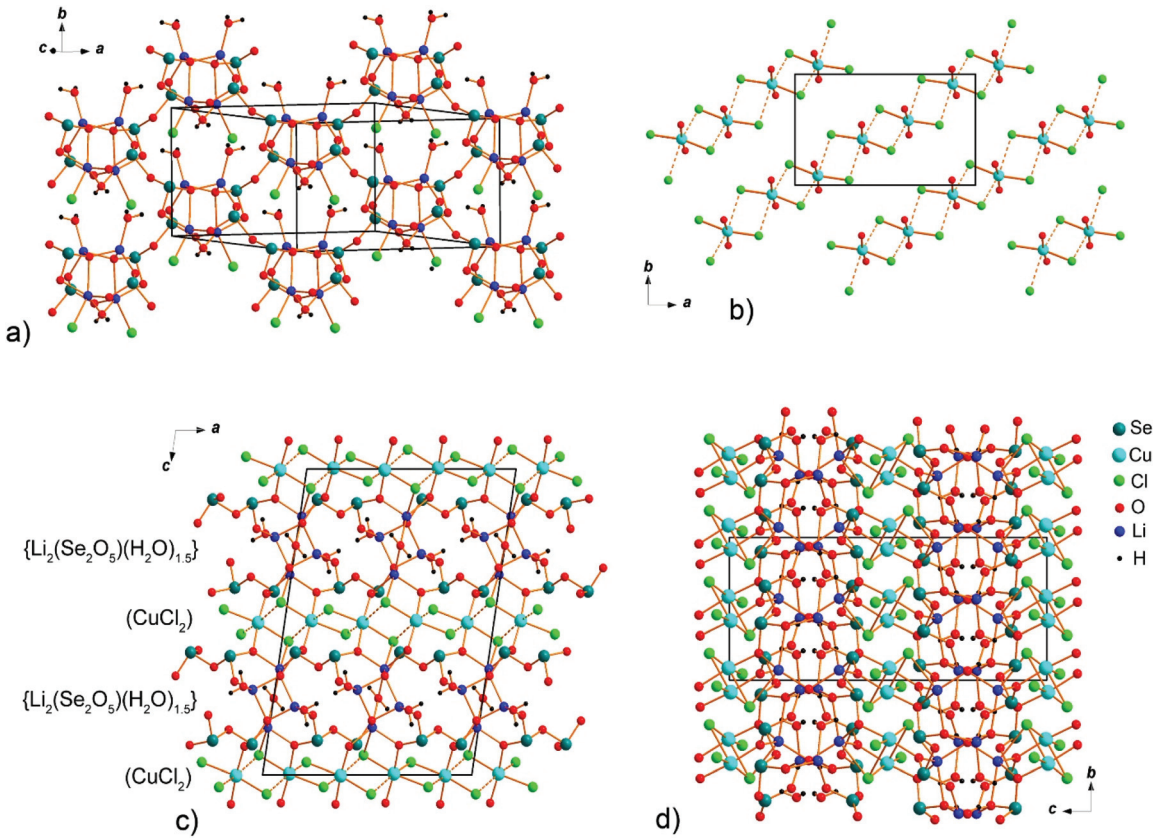

Fig. 4 $\{Li_2(Se_2O_5)(H_2O)_{1.5}\}$ slabs (a) and $CuCl_2$ species (b) in the structure of $Li_2(Se_2O_5)(H_2O)_{1.5}{\cdot}CuCl_2$. General projection of the crystal structure of $Li_2(Se_2O_5)(H_2O)_{1.5}{\cdot}CuCl_2$ along the *b* and *a* axes (c and d).

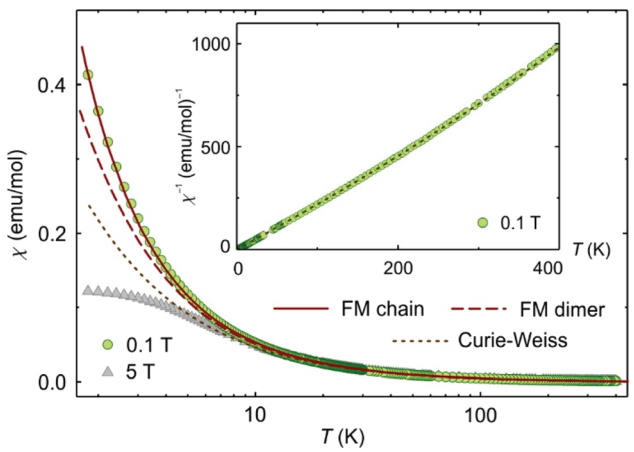

Fig. 5 Temperature dependence of the magnetic susceptibility (main figure) and inverse susceptibility (inset) for $Li_2(Se_2O_5)(H_2O)_{1.5}{\cdot}CuCl_2$ measured in the applied fields of 0.1 and 5 T. The lines show fits of the experimental data: dotted – modified Curie–Weiss law; dashed – ferromagnetic spin dimer (J = −4.4 K, g = 2.22), solid – ferromagnetic spin chain (J = −2.2 K, g = 2.25).

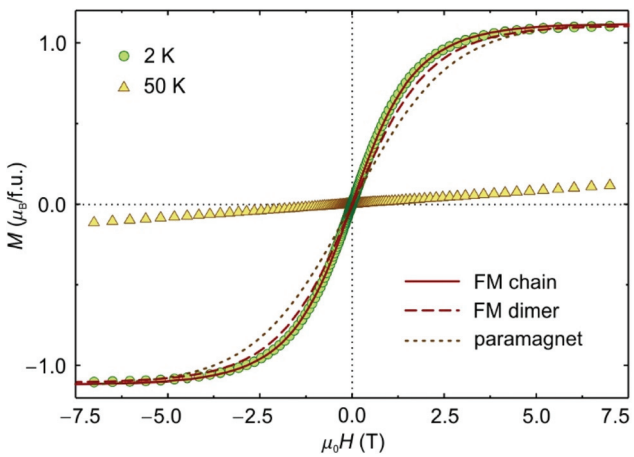

Fig. 6 Field-dependent magnetization of $Li_2(Se_2O_5)(H_2O)_{1.5}{\cdot}CuCl_2$ measured at 2 and 50 K. The solid, dashed, and dotted lines stand, respectively, for the ferromagnetic spin chain with J = −2.2 K, ferromagnetic spin dimer with J = −4.4 K, and paramagnet, all at T = 2 K.

The shortest distance of 3.581(4) Å between the Cu^{2+} ions connects them into magnetic dimers. A longer Cu–Cu contact of 4.086(4) Å further connects these dimers into chains arranged along the crystallographic [110] direction (Fig. 4b). We thus consider two limiting cases: (i) ferromagnetic spin dimers formed by the shorter Cu–Cu contact, and (ii) ferromagnetic spin chains with the same exchange coupling J for both contacts. Already the dimer model with J = −4.4 K

improves the description of the magnetic susceptibility at low temperatures (Fig. 5), but only the chain model with $J = -2.2$ K leads to an accurate description in the whole temperature range down to 2 K and reproduces the experimental magnetization curve as well (Fig. 6). The results for an alternating spin chain, where the coupling is weaker for the longer contact and stronger for the shorter contact, are intermediate between the two. The best agreement found for the limiting case of the uniform spin chain implies that the two Cu–Cu contacts produce interactions of similar strength, even though their Cu–Cu distances differ by 0.5 Å.

Weak ferromagnetic interactions distinguish $Li_2(Se_2O_5)(H_2O)_{1.5}{\cdot}CuCl_2$ from the "layered hydroselenites"[3,4,17] that demonstrate predominantly antiferromagnetic behavior. This difference can be traced back to the different local environment of Cu^{2+}. In $Li_2(Se_2O_5)(H_2O)_{1.5}{\cdot}CuCl_2$, the half-filled magnetically active orbital coincides with the CuO_2Cl_2 plane, which is formed by the shortest Cu–O and Cu–Cl bonds. This arrangement hinders superexchange interactions between the neighboring Cu^{2+} ions, because each Cu–Cl–Cu bridge entails one shorter and one longer Cu–Cl bond (Fig. 4b), with only the former leading to a sizable overlap between the magnetic orbital of Cu^{2+} and p-orbitals of Cl. This scenario is different from the one commonly seen in Cu^{2+} halides, where Cu–Cl–Cu bridges comprise two shorter Cu–Cl bonds, and a strong superexchange interactions controlled by the Cu–Cl–Cu angle ensues.[18,19] On the other hand, Cu^{2+} halides with the one-short-one-long bridges show only weak and usually ferromagnetic couplings on the order of several K.[20,21] A similar superexchange scenario has been reported for oxyhalides, such as $(CuCl)LaNb_2O_7$ with weakly ferromagnetic interactions between the parallel CuO_2Cl_2 plaquettes.[22,23]

Chemical remarks

In the majority of compounds formed in acidic media containing Cu(II) and selenious acid, Se(IV) is present in the form of the hydrogen selenite ion, $HSeO_3^-$.[6] In general, the fate of this anion in the solution may follow several possible routes: (i) incorporation into the structure of strongly bonded complexes; (ii) disproportionation into aqueous H_2SeO_3 and SeO_3^{2-}, which contributes to the formation of poorly soluble selenites, as illustrated by the formation of the by-product, $CuSeO_3{\cdot}2H_2O$, in most of the syntheses described therein; and (iii) dimerization into diselenite anion, $Se_2O_5^{2-}$, as observed *e.g.* for some compounds of calcium;[24] note that this reaction is dominant in the chemistry of sulfur, the earlier analog of selenium. The only compound containing both HSO_3^- and SO_3^{2-} is anhydrous.[25] On the contrary, the equilibrium $2HSeO_3^- \leftrightarrow Se_2O_5^{2-} + H_2O$ is likely to be very dynamic, since the diselenite anions and water molecules do coexist in the solid state. To the best of our knowledge, $Li_2(Se_2O_5)(H_2O)_{1.5}{\cdot}CuCl_2$ is the first example of diselenite hydrate and, moreover, hydrated copper(II) diselenite as well. Most likely, this becomes possible due to the presence of the templating Li^+(aq.) species.

Conclusion

As expected, Li^+ does not contribute to the very flexible (MX)$[Cu(HSeO_3)_2]$ motif, but gives rise to a relatively complex and unique structure. First, it contains both diselenite anions and coordinated water, which has not been observed before. Second, it contains chains of the CuO_2Cl_4 octahedra that strongly resemble the structure of $CuCl_2{\cdot}2H_2O$. The analogous copper bromide hydrate is not known to date, which may also explain our inability to prepare the bromide analogue of $Li_2(Se_2O_5)(H_2O)_{1.5}{\cdot}CuCl_2$. In addition, the alignment of chains in $Li_2(Se_2O_5)(H_2O)_{1.5}{\cdot}CuCl_2$ and cupric chloride dihydrate have much in common. The structure of $Li_2(Se_2O_5)(H_2O)_{1.5}{\cdot}CuCl_2$ therefore bears essential resemblance to the host–guest and salt inclusion structures common for the lone-pair cations.[26] Similar to (MX)$[Cu(HSeO_3)_2]$, there is a complete spatial separation of Li^+ and Cu^{2+}, whereas the Cl^- and Se^{IV} species are arranged more evenly. The complex and relatively porous architecture of $Li_2(Se_2O_5)(H_2O)_{1.5}{\cdot}CuCl_2$ may be the reason for its relatively low stability, which is manifested by the very long crystallization (probably nucleation) time and easy dissolutive decomposition, as well as intolerance towards substitution of Cl^- by Br^-. $Li_2(Se_2O_5)(H_2O)_{1.5}{\cdot}CuCl_2$ is evidently not the least stable compound among hydrated lithium – copper selenite halides as indicated by the elusive behavior of the red crystals mentioned above. Synthesis of further compounds of this series may help in elucidating the structural trends in this unusual and rather dynamic system.

Conflicts of interest

There are no conflicts to declare.

Acknowledgements

This work was financially supported by the Russian Foundation for Basic Research, Grant No. 19-05-00413. Technical support by the SPbSU Resource Centers is gratefully acknowledged. AAT was supported by Federal Ministry for Education and Research through the Sofja Kovalevskaya Award of Alexander von Humboldt Foundation.

Notes and references

1 I. Zimmermann and M. Johnsson, *Cryst. Growth Des.*, 2014, **14**, 5252–5259.
2 V. M. Kovrugin, M. Colmont, O. I. Siidra, V. V. Gurzhiy, S. V. Krivovichev and O. Mentré, *J. Cryst. Growth*, 2017, **457**, 307–313.
3 A. M. Lafront and J. C. Trombe, *Inorg. Chim. Acta*, 1995, **234**, 19–25; A. M. Lafront, J. C. Trombe and J. Bonvoisin, *Inorg. Chim. Acta*, 1995, **238**, 15–22.
4 J. C. Trombe, A. M. Lafront and J. Bonvoisin, *Inorg. Chim. Acta*, 1997, **262**, 47–51.

5 V. M. Kovrugin, S. V. Krivovichev, O. Mentré and M. Colmont, *Z. Kristallogr. – Cryst. Mater.*, 2015, **230**, 573–577.
6 D. O. Charkin, M. R. Markovski, O. I. Siidra and D. O. Nekrasova, *Z. Kristallogr. – Cryst. Mater.*, 2019, **234**, 739–747.
7 M. R. Markovski, D. O. Charkin, O. I. Siidra and D. O. Nekrasova, *Z. Kristallogr. – Cryst. Mater.*, 2019, **234**, 749–756.
8 G. M. Sheldrick, *Acta Crystallogr., Sect. C: Struct. Chem.*, 2015, **71**, 3–8.
9 J. Kretzschmar, N. Jordan, E. Brendler, S. Tsushima, C. Franzen, H. Foerstendorf and V. Brendler, *Dalton Trans.*, 2015, **44**, 10508–10515.
10 E. A. Secco, *Can. J. Chem.*, 1988, **66**, 329–336.
11 S. Todo and K. Kato, *Phys. Rev. Lett.*, 2001, **87**, 047203.
12 A. F. Albuquerque, *et al.* (ALPS collaboration), *J. Magn. Magn. Mater.*, 2007, **310**, 1187.
13 H. W. Lerner and M. Bolte, *Acta Crystallogr., Sect. E: Crystallogr. Commun.*, 2003, **59**, i20–i21.
14 S. Brownstein, N. F. Han, E. J. Gabe and Y. Le Page, *Z. Kristallogr. – Cryst. Mater.*, 1989, **189**, 13–15.
15 G. A. Bain and J. F. Berry, *J. Chem. Edu.*, 2008, **85**, 532–536.
16 A. Abragam and B. Bleaney, *Electron paramagnetic resonance of transition ions*, Clarendon Press, Oxford, 1970.
17 T. Asai and R. Kiriyama, *Bull. Chem. Soc. Jpn.*, 1973, **46**, 2395–2401.
18 W. E. Estes, J. R. Wasson, J. W. Hall and W. E. Hatfield, *Inorg. Chem.*, 1978, **17**, 3657–3664.
19 M. Rodriguez, A. Llobet, M. Corbella, A. E. Martell and J. Reibenspies, *Inorg. Chem.*, 1999, **38**, 2328–2334.
20 M. Megnamisi-Belombe and M. A. Novotny, *Inorg. Chem.*, 1980, **19**, 2470–2473.
21 S. K. Hoffmann, D. K. Towle and W. E. Hatfield, *Mol. Cryst. Liq. Cryst.*, 1984, **107**, 161–170.
22 A. A. Tsirlin and H. Rosner, *Phys. Rev. B: Condens. Matter Mater. Phys.*, 2010, **82**, 060409(R).
23 C. Tassel, J. Kang, C. Lee, O. Hernandez, Y. Qiu, W. Paulus, E. Collet, B. Lake, T. Guidi, M.-H. Whangbo, C. Ritter, H. Kageyama and S.-H. Lee, *Phys. Rev. Lett.*, 2010, **105**, 167205.
24 J. Valkonen, *J. Solid State Chem.*, 1986, **65**, 363–369.
25 A. Magnusson, L. G. Johansson and O. Lindqvist, *Acta Crystallogr., Sect. C: Cryst. Struct. Commun.*, 1983, **39**, 819–822.
26 I. D. Kharitonov, D. O. Charkin, P. S. Berdonosov, C. Black, L. J. Downie, P. Lightfoot and V. A. Dolgikh, *Eur. J. Inorg. Chem.*, 2014, **19**, 3140–3146.
27 O. C. Gagné and F. C. Hawthorne, *Acta Crystallogr., Sect. B: Struct. Sci., Cryst. Eng. Mater.*, 2015, **71**, 562–578.
28 N. E. Brese and M. O'Keeffe, *Acta Crystallogr., Sect. B: Struct. Sci.*, 1991, **47**, 192–197.